Limnol. Oceanogr., 53(4), 2008, 1266–1278

Inorganic carbon uptake by Southern Ocean phytoplankton

Philippe D. Tortell
Department of Earth and Ocean Sciences, University of British Columbia, 6270 University Blvd., Vancouver, British Columbia V6T 1Z4, Canada; Department of Botany, University of British Columbia, 6270 University Blvd., Vancouver, British Columbia V6T 1Z4, Canada

Chris Payne and Celine Gueguen[1]
Department of Earth and Ocean Sciences, University of British Columbia, 6270 University Blvd., Vancouver, British Columbia V6T 1Z4, Canada

Robert F. Strzepek and Philip W. Boyd
Department of Chemistry, University of Otago, P.O. Box 56, Dunedin, 9003, New Zealand; National Institute of Water and Atmospheric Research, Department of Chemistry, University of Otago, P.O. Box 56, Dunedin, 9016, New Zealand

Björn Rost
Alfred Wegener Institute for Polar and Marine Research, Handelshaven 12, D-27515 Bremerhaven, Germany

Abstract

We report the results of laboratory and field studies examining inorganic carbon (C_i) utilization by Southern Ocean phytoplankton. Both in monospecific laboratory cultures of diatoms and *Phaeocystis antarctica* and in natural assemblages in the Ross Sea, C_i uptake by phytoplankton was dominated by direct HCO_3^- transport. The contribution of HCO_3^- transport to total C_i uptake ranged from 65% to 95%, with an overall average of ~80%. There was no significant difference among diatoms and *Phaeocystis* in the extent of HCO_3^- transport. Extracellular carbonic anhydrase activity (eCA) was detected in eight of nine laboratory phytoplankton cultures and in all natural assemblages in the Ross Sea. The effective catalytic enhancement of $HCO_3^-:CO_2$ interconversion ranged from 1.5- to 13-fold (overall mean ~4-fold). Diatom-dominated Ross Sea assemblages had significantly greater eCA levels than did *Phaeocystis*-dominated assemblages. We found no strong correlations between C_i uptake parameters and in situ CO_2 concentrations or chlorophyll *a* levels in the Ross Sea assemblages. Incubation experiments with natural assemblages showed that HCO_3^- uptake and eCA expression did not change significantly over an 8-fold range in pCO_2 (10.1–81.1 Pa), although total short-term C fixation rates increased under low CO_2 conditions. Carbon-concentrating mechanisms are widespread among Southern Ocean phytoplankton and constitutively expressed by natural assemblages in the Ross Sea.

In recent years, there has been a concerted effort to understand the factors controlling phytoplankton growth in the Southern Ocean. This region exerts a disproportionately large influence on the marine carbon cycle (Schlitzer 2002), and plays an important role in regulating atmospheric CO_2 concentrations (Sigman and Boyle 2000). Although primary productivity is strongly Fe-limited across much of the Southern Ocean (Boyd 2002), seasonal diatom blooms occur in specific regions subject to natural iron fertilization (de Baar et al. 1995). In addition, diatoms and the colonial haptophyte *Phaeocystis antarctica* form extensive blooms in coastal and marginal regions such as the Ross Sea (Smith and Asper 2001). These large blooms contribute significantly to overall Southern Ocean productivity (Arrigo and Van Dijken 2007) and can serve as highly efficient vectors of vertical particulate carbon flux to subsurface waters (DiTullio et al. 2000).

Southern Ocean diatoms and *Phaeocystis* have distinct effects on surface ocean biogeochemical cycles. Whereas diatoms have a unique requirement for Si, *Phaeocystis* appears to have elevated N : P and C : P ratios (Arrigo et al. 1999). In addition, *Phaeocystis* is known to be a prolific producer of dimethylsulfoniopropionate (Keller et al. 1989), the precursor compound to the climatologically important gas dimethylsulfide (DMS). Changes in the relative abundance of Antarctic diatoms and *Phaeocystis* thus have potentially important oceanographic implications. Intensive field studies conducted during the Joint Global Ocean Flux Study (Smith et al. 2000) coupled with satellite observations (Arrigo and Van Dijken 2004) have examined the environmental factors regulating the relative biomass and productivity of diatoms and *Phaeocystis* in the

[1] Current address: Department of Chemistry, Trent University, 1600 West Bank Dr., Peterborough, Ontario K9J 7B8, Canada.

Acknowledgments

We thank the captain and scientific crew of the NB *Palmer* for logistical assistance, and Klaus-Uwe Richter and Robert van Hale for assistance in the laboratory. Julie Rose kindly provided one of the *Phaeocystis* strains used for culture experiments. We also thank two anonymous reviewers for detailed and insightful comments.

Funding for this work was provided by grants from the Natural Sciences and Engineering Research Council of Canada (P.D.T.), the Foundation for Research Science & Technology, New Zealand (R.F.S., P.W.B.), and the US National Science Foundation (NSF-OPP-0338097).

Ross Sea. Much of this work has focused on sea-ice cover, mixed-layer depth, and Fe supply as key ecological determinants (Sedwick and DiTullio 1997; Arrigo et al. 1999). The annual retreat and melting of sea ice appears to exert primary controls on phytoplankton productivity (Arrigo and Van Dijken 2004), while also affecting surface water mixed-layer depths and iron supply (Sedwick and DiTullio 1997). In turn, mixed-layer depth and iron availability are believed to influence the relative abundance of diatoms and *Phaeocystis* (Sedwick and DiTullio 1997; Arrigo et al. 1999).

In addition to Fe and light availability, Southern Ocean pCO_2 levels also exhibits strong seasonal variability. In the Ross Sea, for example, pCO_2 ranges from significantly supersaturated wintertime values to some of the lowest levels reported for oceanic waters during intense spring and summer blooms (Bates et al. 1998). The potential effects of this CO_2 variability on primary productivity have thus far not been examined. Recent field studies have demonstrated, however, that phytoplankton in midlatitude oceanic waters are physiologically sensitive to CO_2. Short-term experiments have provided evidence for a small but significant CO_2 effect on C fixation over 12 h (Hein and Sand-Jensen 1997) and large changes in the expression of several key C assimilation enzymes (e.g., RubisCO and carbonic anhydrase) over 1–3 d (Tortell et al. 2000). Over longer timescales, CO_2 concentrations have also been shown to influence the species composition of marine phytoplankton assemblages. Experiments conducted in the equatorial Pacific demonstrated a significant CO_2-dependent change in the relative abundance of diatoms and *Phaeocystis pouchetii*, with diatom abundance increasing under high CO_2 conditions (Tortell et al. 2002). The physiological basis for this result and the extent to which it applies to the mixed diatom and *Phaeocystis* assemblages in the Ross Sea are presently unknown.

Understanding potential CO_2 effects on marine phytoplankton requires knowledge of the physiological mechanisms of cellular C uptake and fixation. Early laboratory culture experiments suggested that some large Antarctic diatoms could be growth limited by diffusive CO_2 supply (Riebesell et al. 1993), but subsequent studies demonstrated the widespread occurrence of inorganic carbon-concentrating mechanisms (CCMs) in a variety of marine phytoplankton species and natural assemblages (Tortell et al. 2000; Giordano et al. 2005; Martin and Tortell 2006). The CCM acts to increase the efficiency of net C fixation by concentrating CO_2 in the vicinity of RubisCO and repressing the enzyme's oxygenase activity. This is achieved through the active uptake of HCO_3^- and/or CO_2, the expression of carbonic anhydrase (which catalyzes $HCO_3^- : CO_2$ interconversion), and, in at least some diatom species, a C_4-like C assimilation pathway (Reinfelder et al. 2004).

To date, very few studies have examined the physiological mechanisms of inorganic C acquisition by Southern Ocean phytoplankton or their response to CO_2 variability. The first evidence for CCM activity in Antarctic microalgae came from the laboratory studies of Mitchell and Beardall (1996) with the sea-ice diatom *Nitzschia frigida*. More recently, Cassar et al. (2004) have reported measurements of CCM activity in mixed phytoplankton assemblages of the Antarctic Polar Frontal Zone. No work has thus far examined phytoplankton C acquisition in high-productivity coastal regions of the Southern Ocean, or explicitly compared the pathways of C utilization by Antarctic diatoms and *Phaeocystis*. Stable C isotope data suggest, however, that there are significant differences in C uptake between these taxonomic groups (Villinski et al. 2000). Here we present the results of laboratory and field experiments examining inorganic C uptake by Southern Ocean phytoplankton. Laboratory culture experiments were designed to measure the relative contribution of HCO_3^- and CO_2 as photosynthetic C sources for *P. antarctica* and seven Antarctic diatom species, and field studies examined HCO_3^- and CO_2 transport in Ross Sea assemblages and extracellular carbonic anhydrase activity (eCA). Our study was aimed at elucidating the differences in C acquisition between diatoms and *Phaeocystis*, and examining the effects of natural and anthropogenic CO_2 variability on phytoplankton C uptake in the Ross Sea.

Methods

Laboratory phytoplankton culturing—We cultured a number of phytoplankton isolates under controlled laboratory conditions for use in C uptake experiments. The species used for laboratory experiments had been previously isolated from the Southern Ocean, and included seven diatoms (both pennate and centric) as well as two strains of *P. antarctica*. The diatoms used for experiments were *Fragilariopsis cylindrus*, *Fragilariopsis curta*, *Rhizoselenia* spp., *Chaetoceros* spp., *Eucampia antarctica*, *Thalassiosira* spp., and *Nitzschia* spp. Although *P. antarctica* is known to grow both in colonial form and as individual flagellated cells, all of our experiments were conducted with colonies, which ranged in size from ~400 to 2,000 μm in diameter.

All phytoplankton species were maintained in semi-continuous batch cultures (300–800-mL culture vessels) at growth temperatures of 4°C. For all species except one of the *Phaeocystis* isolates (designated as "Otago"), the culturing medium was natural Southern Ocean water amended with f/20 trace metals and macronutrients. The Otago *Phaeocystis* isolate was cultured using synthetic ocean water amended with AQUIL vitamins, nutrients, and trace metals (Price et al. 1988). All species were grown under trace-metal–replete conditions. Continuous illumination was provided by artificial lighting (300 μmol quanta m^{-2} s^{-1}), and except for the Otago *Phaeocystis*, cultures were bubbled with laboratory air. After the cultures had been allowed to acclimate for several transfers (>10 generations), cells growing in exponential phase were harvested by gentle filtration onto 2.0-μm polycarbonate membranes and immediately resuspended into the pH 8.5 seawater buffer (10 mmol L^{-1} Bicine) for ^{14}C fixation experiments (*see* below). For some experiments, 20 μmol L^{-1} acetazolamide (AZ) (Sigma Chemical) was used to inhibit extracellular carbonic anhydrase activity, whereas other experiments were run with 100 μmol L^{-1}

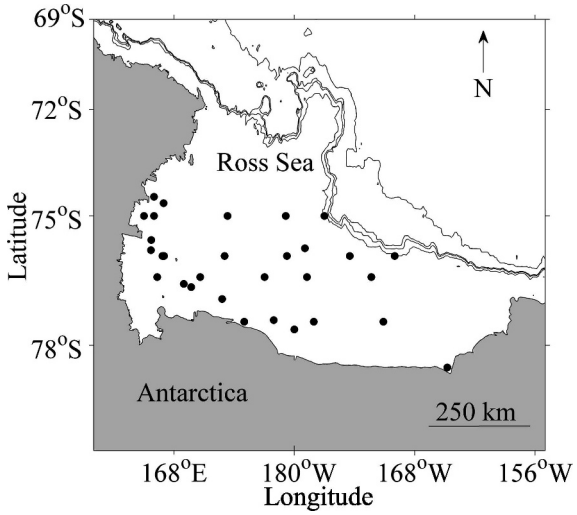

Fig. 1. Location of sampling stations in the Ross Sea, Dec 2005–Jan 2006. Depth contours represent the 1,000-, 1,400-, 1,600-, and 3,000-m isobaths.

dextran-bound sulfanilamide (DBS) (Ramidus AB). Both DBS and AZ are equally effective in inhibiting eCA. The inhibitors were added at least 10 min prior to the start of experiments.

Field sampling—Surface seawater samples (5 m) were collected from a variety of locations (Fig. 1) in the Ross Sea during austral summer (Dec 2005–Jan 2006; RV *Nathaniel B. Palmer*, cruise 06-01). At each site, chlorophyll *a* (Chl *a*) concentrations were determined by fluorometric analysis (Parsons et al. 1984), nutrient concentrations were determined by autoanalyzer (Gordon et al. 1993), and CO_2 levels were measured by membrane inlet mass spectrometry (MIMS) (Tortell 2005). Temperature and salinity data were obtained from a conductivity, temperature, depth (CTD) profiler and the ship's underway thermosalinograph system. Phytoplankton assemblage composition was qualitatively assessed by microscopic examination of concentrated samples preserved with 1% (final concentration) glutaraldehyde.

To collect natural phytoplankton assemblages for in vivo C fixation measurements, a 20-liter seawater sample was dispensed from Niskin bottles into a polypropylene carboy and immediately transferred to a 4°C walk-in cooler. Phytoplankton were concentrated from the seawater by gravity filtration onto 47-mm, 2.0-μm–pore size polycarbonate membranes (four filters were run in parallel). In many cases, the filters clogged before the entire 20 liters was utilized. Material collected onto the filters was then resuspended into either a pH 8.5 buffer (20 mmol L^{-1} Bicine in 0.2-μm-filtered seawater) for isotope disequilibrium experiments, or a pH 8.25 buffer (10 mmol L^{-1} Bicine in 0.2-μm-filtered seawater) for eCA assays (*see* below). The final concentration of Chl *a* in cell concentrates ranged from 0.1 to 4 mg L^{-1}. Experiments were begun within 15 min of resuspending cells in the buffers.

CO_2 manipulation experiment—In addition to in situ sampling, we also conducted an incubation experiment to specifically examine the CO_2-dependent regulation of C uptake by the Ross Sea phytoplankton assemblages. The experiment was conducted using the semi-continuous batch culture technique described by Tortell et al. (2002), in which phytoplankton cultures are periodically diluted with filtered water to extend the timescale of the exponential growth phase. Surface seawater (~5 m) for the incubation experiment was collected at 74.56°S, 174.48°W in the Ross Sea polynya using a trace-metal–clean in situ pumping system. Approximately 50 liters of unfiltered water was collected into a single trace-metal–clean carboy and dispensed in nine 4-liter acid-cleaned polycarbonate bottles equipped with custom-made gas inflow and sampling ports. An additional ~200 liters of 0.2-μm-filtered water was collected for subsequent dilution of samples. Triplicate bottles were utilized for each of three CO_2 treatment levels; 10.1, 35.5, and 81.1 Pa (equivalent to 100, 380, and 800 ppm). The CO_2 concentration in sample bottles was adjusted by continuous bubbling of the seawater with commercial gas mixtures (Scott Specialty Gases) containing the desired CO_2 partial pressures blended into an air-balance gas. Bottles were placed in a flow-through seawater tank on the ship's deck, maintaining a temperature of ±1°C of ambient sea surface values. Two layers of neutral density screening were used to reduce light to ~30% of surface irradiance. To eliminate potential Fe limitation of indigenous phytoplankton, 1 nmol L^{-1} Fe (as $FeCl_2$) was added to all bottles and dilution water. No other macronutrients were added to bottles.

Phytoplankton growth during the incubation experiment was monitored by daily measurements of Chl *a* concentrations and major nutrient drawdown (both measured as described above). When major nutrients reached ~10% of starting values, approximately 90% of the sample volume was removed from each bottle for experiments and replaced with the filtered dilution water. The phytoplankton samples removed from incubation bottles were gravity-filtered onto 2.0-μm membranes and resuspended in experimental buffers for isotope disequilibrium experiments and/or the analysis of extracellular carbonic anhydrase. Replicate samples from individual bottles within a CO_2 treatment were pooled for isotope disequilibrium measurements, and individual bottle replicates were analyzed for eCA. The maximum phytoplankton biomass achieved in the incubation was ~15 μg Chl *a* L^{-1}, and the experiment was run for 8 d.

^{14}C experiments—The isotope disequilibrium technique was used to determine the relative fraction of HCO_3^- and CO_2 uptake in concentrated cell suspensions. This method has been extensively described in several recent articles, to which the reader is referred for full details of the protocol and data analysis (Elzenga et al. 2000; Tortell and Morel 2002; Martin and Tortell 2006). Essentially, short-term cellular ^{14}C fixation is monitored during a transient disequilibrium between $^{14}CO_2$ and $H^{14}CO_3^-$ in solution. During experiments, the specific activity of CO_2 decreases exponentially by a factor of ~70, whereas the specific activity of the combined $HCO_3^- : CO_3^{-2}$ pool is essentially constant. The time course of ^{14}C fixation reflects the specific activity of intracellular CO_2 and HCO_3^- pools,

which in turn reflect the relative proportion of these substrates transported across the cellular membrane (Espie and Colman 1986). The fraction of HCO_3^- uptake, f, is related to the degree of curvature in the time-course data. Cells that only take up HCO_3^-—either through a direct transport mechanism or via extracellular carbonic anhydrase-catalyzed conversion to CO_2—exhibit nearly linear time-course kinetics. In contrast, cells taking up only CO_2 show a high degree of curvature in ^{14}C accumulation, which reflects the large decrease in the CO_2 specific activity during the time course (Martin and Tortell 2006).

To perform experiments, aliquots of concentrated cell suspensions (2.5 mL) were transferred into a temperature-controlled (2.0°C), illuminated (500 μE m^{-2} s^{-1} photosynthetically active radiation) cuvette and allowed to acclimate for several minutes. A pH 7.0 ^{14}C spike was then added to the concentrated cell suspensions to yield a final specific activity of ~1 μCi μmol C^{-1}. (The ^{14}C addition contributed an additional ~1 μmol of inorganic carbon (C_i) to the seawater buffer, less than 1% of the background concentration.) To prepare the ^{14}C spike, 10 μCi of radioisotope stock solution (55 μCi μmol^{-1}, Cat. No. CAF3, GE Health Sciences) was diluted 10 : 1 into a 50 mmol L^{-1} Hepes buffer. After the initial ^{14}C addition, subsamples (200 μL) were withdrawn from the cuvette with a pipette and transferred at short intervals into 7-mL scintillation vials containing 1 mL of 6 mol L^{-1} HCl. This procedure effectively terminated photosynthesis and converted all unfixed (i.e., inorganic) ^{14}C into CO_2, which was degassed from samples by placing the scintillation vials on an orbital platform shaker (~40 rpm) for at least 12 h. Total organic ^{14}C in degassed samples was quantified by liquid scintillation counting on a Beckman LS6500 counter using quench correction to calculate disintegrations per minute (DPM). We used 5 mL of scintillation cocktail (Fisher Scintisafe) for all samples.

To extract quantitative estimates for HCO_3^- uptake ($fHCO_3^-$) and extracellular carbonic anhydrase expression from the isotope disequilibrium results, we fit the ^{14}C time-course data to the equations presented in Martin and Tortell (2006) using the Marquand-Levenberg nonlinear regression algorithm in SigmaPlot. This algorithm provides least squares parameter estimates and standard errors. When extracellular carbonic anhydrase is inhibited, the rate constant of extracellular $CO_2 : HCO_3^-$ interconversion is known, and the ^{14}C time course can be interpreted strictly in terms of C transport across the cell membrane (Martin and Tortell 2006). For control experiments without inhibitor treatment, eCA is derived by including an additional free parameter (α') in the curve-fitting procedure representing the rate of extracellular $CO_2 : HCO_3^-$ interconversion. Comparison of model-derived α' values with the uncatalyzed thermodynamic rate constant (Espie and Colman 1986) allows the calculation of a relative enhancement factor defined as ($\alpha' : \alpha$), where α' and α are the rates of $HCO_3^- : CO_2$ interconversion in the presence and absence of cells, respectively. When extracellular carbonic anhydrase expression is explicitly included in the model, $fHCO_3^-$ represents direct HCO_3^- transport by cells untreated with inhibitors.

MIMS—Extracellular CA activity was also directly measured in the majority of our field samples using MIMS. Concentrated cell suspensions in a pH 8.25 buffer (10 mmol L^{-1} Bicine, 0.2 μm filtered seawater) were placed in a darkened, thermostatted cuvette (2.5°C) connected to a quadrupole mass spectrometer (HAL 3F/HPR 40, Hiden Analytical) via a silicone membrane inlet (Tortell et al. 2006). Carbonic anhydrase activity was measured by following the time course of ^{18}O loss from $^{13}C^{18}O_2$ through exchange with background $H_2{}^{16}O$ (Badger and Price 1989). The mass spectrometer was set to measure masses 49 ($^{13}C^{18}O^{18}O$), 47 ($^{13}C^{18}O^{16}O$), and 45 ($^{13}C^{16}O^{16}O$) every 3 s, and the $HCO_3^- : CO_2$ interconversion rate was quantified by calculating the rate of ^{18}O loss from the ^{13}C-labeled CO_2 pool (and hence disappearance of the mass 49 CO_2 species). Background rates of uncatalyzed $HCO_3^- : CO_2$ interconversion were determined periodically using cell-free buffer. Enzyme activity units were calculated as:

$$U = S_c/S_u - 1 \quad (1)$$

where S_c is the catalyzed rate (i.e., in the presence of the sample) and S_u is the uncatalyzed (i.e., blank) rate in cell-free buffer. Using this formulation, one unit of activity reflects a 100% enhancement of the ^{18}O loss rate relative to the uncatalyzed value. These enzyme activities were normalized to the Chl *a* content cell suspensions as measured in 100-μL aliquots. Chl *a* was measured fluorometrically following at least 24-h extraction in −20°C acetone (Parsons et al. 1984). For most samples, we examined the effects of DBS additions on apparent eCA in the MIMS assays. The inhibitor was added to concentrated samples at a final concentration of 100 μmol L^{-1} after an initial catalytic rate had been established for at least 15 min. Unfortunately, because of technical problems with the mass spectrometer, extracellular carbonic anhydrase measurements could not be made for the last six sampling stations in our Ross Sea survey.

Results

Ross Sea biological and hydrographic conditions—The general characteristics of our Ross Sea sampling sites are presented in Table 1. Chl *a* concentrations ranged from 0.7 to 5.2 μg L^{-1}, with the majority of the biomass at most stations falling into the large (i.e., >20 μm) size class. Macronutrient concentrations were generally high across the entire sampling region, with only three stations having NO_3^- levels less than 2 μmol L^{-1}. At all stations, surface water pCO_2 was undersaturated relative to atmospheric equilibrium, with minimum values of 12.8 Pa (126 ppm). Temperature ranged from −1°C to 3°C, and salinity ranged from 33.12 to 34.52. Phytoplankton communities were composed of a mixture of diatoms and *P. antarctica*. Prevalent diatom genera included *Fragilariopsis*, *Pseudo-nitzschia*, *Chorethron*, *Chaetoceros*, and *Leptocylindrus*. The majority of *Phaeocystis* occurred in colonial phase (colonies were not well preserved in all fixed samples, but were observed in fresh material collected for experiments). More

Table 1. Ross Sea station locations with biological and chemical characteristics.

Station	Latitude (°S)	Longitude (°E)	Chl *a* (μg L^{-1})	% Chl *a* >20 μm	Dominant phytoplankton*	NO_3 (μmol L^{-1})	SiO_2 (μmol L^{-1})	pCO_2 (Pa)
2	75.815	−178.946	4.32	81	—	16.76	62.49	22.9
5	77.666	−180.000	3.24	28	—	13.88	74.01	19.1
8	77.464	177.933	2.94	51	—	13.02	81.81	17.9
13	77.000	172.800	3.55	39	*Phaeocystis*	14.47	67.51	20.3
18	76.733	169.716	2.15	40	*Phaeocystis*	15.25	82.31	19.2
20	76.500	166.321	0.96	51	—	25.08	80.41	18.8
23	76.500	170.608	1.25	67	—	15.50	72.71	20.0
29	76.500	177.033	1.12	54	mixed†	16.79	72.82	22.1
31	76.500	−178.748	3.54	44	mixed	21.68	76.82	29.0
35	76.500	−172.335	3.44	60	mixed	19.10	72.42	25.4
38	76.000	−170.001	3.01	52	*Phaeocystis*	21.41	78.82	27.5
41	76.000	−174.468	4.82	39	*Phaeocystis*	21.34	81.02	27.2
45	76.000	179.249	1.57	60	mixed	18.39	69.52	25.5
49	76.000	173.038	1.24	47	mixed	23.13	63.49	32.8
53	76.000	166.839	5.24	91	diatoms	0.93	22.79	13.3
54	76.000	166.839	—	—	—	—	—	14.7
55	77.500	175.000	0.93	45	mixed	18.66	79.39	24.3
59	77.500	−178.059	0.89	36	mixed	19.06	74.59	25.9
63	77.500	−171.127	0.88	41	diatoms	15.86	67.39	23.4
66	78.649	−164.750	1.00	39	*Phaeocystis*	21.17	83.85	26.9
68	75.000	−177.011	0.65	40	mixed	25.39	80.15	36.3
71	75.000	179.137	2.11	71	mixed	19.18	59.45	28.1
75	75.000	173.332	0.95	51	mixed	23.07	58.39	32.5
77	76.657	168.974	1.71	—	—	14.18	70.25	22.0
79	75.611	165.724	1.41	37	diatoms	12.34	44.05	19.3
81	75.000	165.000	4.68	60	diatoms	21.00	64.55	29.4
84	74.666	166.967	2.41	15	diatoms	6.09	34.15	19.3
95	75.000	166.000	5.01	64	diatoms	6.35	34.47	17.5
97	74.500	166.000	1.28	53	diatoms	1.88	30.07	12.8
99	76.000	167.000	3.70	57	diatoms	1.09	14.47	16.2
101	75.860	165.700	3.43	54	diatoms	13.45	42.67	14.2

* More detailed taxonomic information is presented in Table 2.
† Significant abundances of both diatoms and *Phaeocystis*.

detailed information on the taxonomic composition of phytoplankton at most stations is given in Table 2.

HCO_3^- vs. CO_2 uptake—Figure 2 shows typical results from isotope disequilibrium experiments. For both *Fragilariopsis* and *Phaeocystis*, results obtained in laboratory and field experiments were qualitatively similar. The time course of ^{14}C fixation for *Fragilariopsis* showed a distinct difference between control and DBS treatments, with significant curvature in the presence of the inhibitor and a near-linear time course for the controls (i.e., nontreated cells). In contrast, both laboratory and field populations of *Phaeocystis* showed only a small effect of extracellular carbonic anhydrase inhibitor additions on ^{14}C fixation. Despite this similarity, the degree of curvature in the ^{14}C time course was higher for the field populations of *Phaeocystis* (Fig. 2d).

The fraction of HCO_3^- uptake (hereafter referred to as $f\,HCO_3^-$) derived from ^{14}C fixation curves is presented in Table 3 for AZ or DBS-treated laboratory cultures and Table 4 for DBS-treated Ross Sea assemblages. Overall, direct HCO_3^- transport dominated C use for all stations and individual species. Values of $f\,HCO_3^-$ in inhibitor-treated cells ranged from 0.64 to 0.91 (mean 0.83 ± 0.01 SE) in field assemblages, and 0.65 to 0.94 (mean 0.80 ± 0.04) in the laboratory cultures. In most cases, parameter estimates (i.e., calculated. $f\,HCO_3^-$ values) had standard errors of <5%, indicating excellent model fit to the data. Comparison of the results in Tables 3 and 4 shows a strong quantitative similarity between laboratory and field measurements. The mean $f\,HCO_3^-$ value derived for *Fragilariopsis*-dominated assemblages (Stas. 29, 45, 53, 55, 59, 63, and 81–101; *see* Table 2) was 0.86 ± .04, in excellent agreement with the value of 0.87 obtained for inhibitor-treated laboratory cultures. For the *Phaeocystis*-dominated assemblages (Stas. 13, 18, 38, 41, and 66), mean $f\,HCO_3^-$ values were 0.82 ± 0.07, and the value obtained for an AZ-treated laboratory culture was 0.94. Given the 95% confidence interval (2σ) of the field measurements (0.68–0.96), these two values are not significantly different. Although all field samples clustered close to the mean $f\,HCO_3^-$ value of 0.83, Sta. 75 appeared to be somewhat exceptional, with an estimated $f\,HCO_3^-$ value of 0.64. This value was, however, associated with a large standard error (±0.11), and thus not statistically different from the overall mean at the 95% confidence level (95% confidence interval = 0.42, 0.86).

Tables 3 and 4 also present $f\,HCO_3^-$ values derived for control experiments in which cells were not treated with

Table 2. Taxonomic information on phytoplankton assemblages. Taxa underlined were numerically dominant.

Station	Dominant phytoplankton taxa
13	*Phaeocystis*, *Pseudonitzschia*, *Fragilariopsis*, *Chaetoceros*
18	*Phaeocystis*, *Chaetoceros*
29	*Fragilariopsis*, *Chaetoceros*, *Phaeocystis*, *Asteromphalus*, *Nitzschia*, *Pseudonitzschia*
31	*Pseudonitzschia*, *Phaeocystis*
35	*Pseudonitzschia*, *Phaeocystis*, *Fragilariopsis*
38	*Phaeocystis*, *Fragilariopsis*
41	*Phaeocystis*, *Fragilariopsis*, *Pseudonitzschia*
45	*Fragilariopsis*, *Pseudonitzschia*, *Phaeocystis*, *Asteromphalus*, *Nitzschia*, *Chaetoceros*
49	*Pseudonitzschia*, *Phaeocystis*, *Fragilariopsis*, *Asteromphalus*, *Chaetoceros*, *Nitzschia*
53	*Fragilariopsis*, *Asteromphalus*, *Pseudonitzschia*
55	*Fragilariopsis*, *Phaeocystis*, *Pseudonitzschia*, *Leptocylindrus*, *Chaetoceros*
59	*Fragilariopsis*, *Chaetoceros*, *Nitzschia*, *Phaeocystis*
63	*Fragilariopsis*, *Nitzschia*, *Pseudonitzschia*, *Chaetoceros*
66	*Phaeocystis*, *Fragilariopsis*, *Pseudonitzschia*
68	*Pseudonitzschia*, *Phaeocystis*, *Fragilariopsis*, *Nitzschia*, *Chaetoceros*
71	*Pseudonitzschia*, *Chaetoceros*, *Fragilariopsis*, *Phaeocystis*, *Leptocylindrus*, *Chorethron*
75*	*Fragilariopsis*, *Chaetoceros*, *Pseudonitzschia*, *Phaeocystis*
79	*Pseudonitzschia*, *Fragilariopsis*, *Leptocylindrus*
81	*Fragilariopsis*, *Pseudonitzschia*, *Nitzschia*, *Chorethron*
84	*Fragilariopsis*, *Pseudonitzschia*
95	*Fragilariopsis*, *Pseudonitzschia*
97	*Fragilariopsis*, *Pseudonitzschia*
99	*Fragilariopsis*, *Leptocylindrus*, *Pseudonitzschia*
101	*Fragilariopsis*, *Pseudonitzschia*, *Leptocylindrus*

* No individual genus appeared numerically dominant at this station.

extracellular carbonic anhydrase inhibitors. Although these estimates are more prone to error because of an additional free parameter in the model fit, we obtained values that were similar to those derived for inhibitor-treated cells. For the field samples, the mean difference in $f\mathrm{HCO}_3^-$ between control and DBS-treated samples was 6%. For the laboratory experiments, the mean difference between treated and untreated cells was 8%. A particularly large discrepancy (~20–25%) was observed between control and inhibitor-treated *Rhizosolenia* (+AZ), *Chaetoceros* (+AZ), and *Thalassiosira* (+DBS) (Table 3). In all cases in which there was a statistically significant difference between control and inhibitor-treated cells, $f\mathrm{HCO}_3^-$ was lower in the presence of the inhibitor.

At several diatom-dominated Ross Sea stations (79, 81, 95, and 99), $f\mathrm{HCO}_3^-$ parameter values in control experiments were associated with very high errors (>100%). This resulted from a lack of curvature in the ^{14}C time course data as illustrated in Fig. 3 for Sta. 95. Such high linearity in the accumulation curves results from a combination of high HCO_3^- transport and/or high eCA (*see* below). In either case, the linearity of the time-course data yields poor model fits (Rost et al. 2007), and the $f\mathrm{HCO}_3^-$ values derived for control experiments at these stations were excluded from our analysis.

Extracellular carbonic anhydrase—The ^{14}C fixation data were also used to estimate cellular extracellular carbonic anhydrase expression. For cells taking up at least some CO_2, extracellular carbonic anhydrase expression will induce a rapid transition from high initial ^{14}C fixation rates to lower steady-state values, as the enriched $^{14}CO_2$ pool quickly equilibrates with the bulk dissolved C_i. This time-dependent change in apparent ^{14}C fixation rates is best illustrated when the ^{14}C fixation curves are transformed into instantaneous rates (DPM s^{-1}) by taking the slope of ^{14}C activity between successive measurement time points (Tortell and Morel 2002). As an example of this approach, Fig. 4 presents transformed ^{14}C fixation data for the *Fragilariopsis*-dominated phytoplankton assemblage at Sta. 63. In the control experiment (i.e., no inhibitors added), ^{14}C fixation rates decrease much more quickly over time to a steady state value than in the DBS treatment, providing prima facie evidence for cellular extracellular carbonic anhydrase expression.

Quantitative estimates of extracellular carbonic anhydrase expression derived from curve fits of the ^{14}C time course data are presented in Tables 3 and 4 for laboratory cultures and natural assemblages, respectively. The results are presented as catalytic enhancement factors (described above), where a value of 1 indicates no detectable eCA. All of the cultured laboratory species except *Rhizosolenia* showed statistically significant eCA, with enhancement factors ranging from 1.6 to 7.8 (mean 3.12). For the field assemblages (Table 4), at least some eCA was detected at all stations, and enhancement factors ranged from 1.7 to 13 (mean 4.0). For most stations, the error associated with the extracellular carbonic anhydrase estimates was relatively small, and the enhancement factors were significantly different from 1. However, enhancement factors could not be reliably quantified at five diatom-dominated stations (79–84, 99, and 101) where control experiments (i.e., −DBS) exhibited a highly linear ^{14}C time course (Fig. 3). Overall, extracellular carbonic anhydrase expression levels estimated from the ^{14}C data were similar for comparable laboratory and field samples. For *Phaeocystis*, eCA derived for monospecific laboratory cultures (2.82 ± 0.42 enhancement factor) were very similar to those derived for natural assemblages (2.45 ± 0.75). For *Fragilariopsis*, we observed significant variability among natural assemblages in enhancement factors. Given this variability, the mean enhancement factor for the natural assemblages (5.38 ± 1.56) was not statistically different (*t*-test, $p = 0.083$, df = 12) from that observed in the laboratory cultures (2.08 ± 0.72).

For many of the Ross Sea stations, additional measurements of in vivo eCA were made using MIMS analysis of ^{18}O exchange reactions in intact cell suspensions. Typical results, shown in Fig. 5 for Sta. 63, clearly show the enhancement of the $\mathrm{HCO}_3^-:\mathrm{CO}_2$ interconversion rate in the presence of cells. The addition of 100 μmol L^1 DBS to the cell suspensions largely eliminated this apparent catalysis, indicating that the observed enhancement was indeed mediated specifically by extracellular carbonic anhydrase. Calculated MIMS eCA are presented in Table 4. The activities ranged from 0.8 to 9.7 U (μg Chl $a)^{-1}$ with a mean of 3.9 ± 0.37 U (μg Chl $a)^{-1}$.

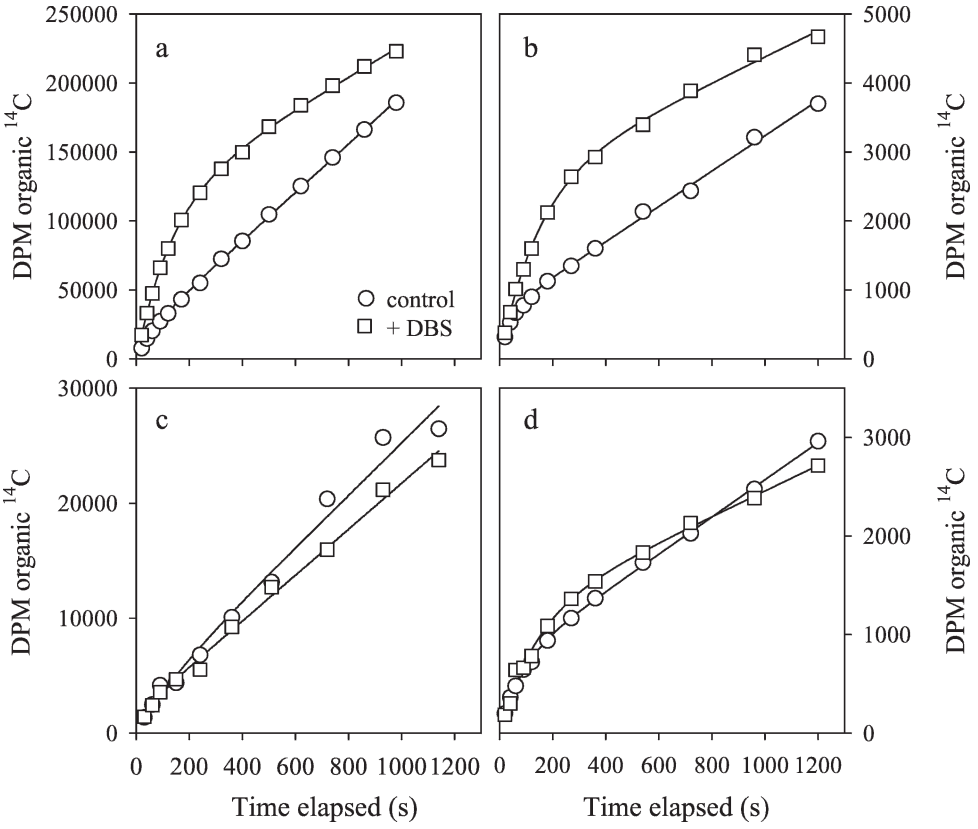

Fig. 2. Results of isotope disequilibrium experiments with laboratory phytoplankton cultures and natural Ross Sea assemblages: (a) laboratory *F. cylindrus*, (b) Ross Sea Sta. 45, (c) laboratory *P. antarctica*, and (d) Ross Sea Sta. 38.

Taxonomic and environmental influences on C acquisition—We examined our dataset for potential relationships between C uptake parameters and various environmental variables. We did not observe any statistically significant correlations between the C uptake parameters and hydrographic variables. Neither $f\mathrm{HCO}_3^-$ nor eCA was correlated to Chl *a* or ambient CO_2 concentrations. To facilitate taxonomic comparisons among our sampling stations, we categorized the Ross Sea assemblages as either diatom-dominated ($\gg$50% diatom abundance), *Phaeocystis*-dominated ($\gg$50% *Phaeocystis* abundance), or mixed, using our qualitative microscopic analysis of samples (Table 2). In our survey, there were 9 diatom-dominated stations, 5 *Phaeocystis*-dominated stations, and 10 stations with mixed assemblages. Taxonomic differences in C uptake parameters are summarized in Table 5. While the mean value of $f\mathrm{HCO}_3^-$ was highest for diatom-dominated assemblages (0.88), the difference in $f\mathrm{HCO}_3^-$ between diatom- and *Phaeocystis*-dominated assemblages was relatively small and not statistically significant (analysis of variance [ANOVA], $p = 0.073$, df = 23). In contrast, there was a large, and statistically significant (ANOVA, $p < 0.001$, df

Table 3. Carbon uptake parameters derived from isotope disequilibrium for laboratory cultures.

Species	eCA inhibitor	*n*	$f\mathrm{HCO}_3^-$+DBS or AZ	$f\mathrm{HCO}_3^-$ control	eCA catalytic enhancement
Fragilariopsis cylindrus	AZ	3	0.86±0.015	0.96±0.01	2.59±0.89
Fragilariopsis curta	AZ	2	0.88±0.014	0.97±0.005	1.57±0.15
Rhizosolenia sp.	AZ	2	0.73±0.116	0.97±0	1.0±0
Chaetoceros sp.	AZ	3	0.67±0.11	0.94±0.01	3.19±2.2
Eucampia antarctica	AZ	3	0.78±0.089	0.87±0.17	1.98±0.66
Thalassiosira sp.	DBS	1*	0.65±0.02	0.82±0.069	7.84±3.52
Nitzschia sp.	DBS	1*	0.84±0.005	0.91±0.01	5.13±0.46
Phaeocystis antarctica	—	2	—	0.83±0.04	2.3±0.23
P. antarctica (Otago)	AZ	3	0.94±0.015	0.95±0.012	2.52±0.91
Mean			0.80±0.04	0.91±0.02	3.12±0.71

* The measurement error is derived from the curve-fitting results (standard error of curve fit).

Table 4. Carbon uptake parameters derived from isotope disequilibrium results with Ross Sea phytoplankton assemblages.

Station	$f\,HCO_3^-$+DBS	$f\,HCO_3^-$ control	eCA catalytic enhancement	eCA (U [μg Chl a]$^{-1}$)
5	—	0.81±0.080	2.3±1.2	—
13	0.83±0.014	0.82±0.034	1.9±0.58	5.1
18	0.72±0.027	0.88±0.019	1.7±0.43	2.7
20	0.88±0.018	0.94±0.005	1.9±0.14	—
29	0.84±0.020	0.88±0.011	4.1±0.43	3.2
31	0.80±0.005	0.78±0.023	6.2±0.72	0.8
35	0.84±0.012	0.76±0.020	5.2±0.58	2.7
38	0.88±0.010	0.92±0.003	1.9±0.14	3.1
41	0.86±0.010	0.85±0.018	3.0±0.58	1.0
45	0.84±0.008	0.86±0.017	3.5±0.58	3.9
49	0.83±0.015	0.89±0.017	3.5±0.72	3.5
53	0.88±0.006	0.91±0.055	13±8.0	3.7
55	0.82±0.017	0.89±0.017	3.0±0.72	3.6
59	0.84±0.015	0.92±0.004	2.5±0.14	4.7
63	0.79±0.022	0.84±0.014	2.3±0.29	4.0
66	0.80±0.023	0.88±0.011	3.2±0.43	2.8
68	0.81±0.006	0.77±0.033	2.5±0.58	4.7
71	0.78±0.015	0.89±0.020	2.9±0.72	2.7
75	0.64±0.114	0.52±0.051	5.7±0.68	9.7
79	0.81±0.005	—	—	7.8
81	0.89±0.003	—	—	—
84	0.90±0.003	0.78±0.205	—	—
95	0.86±0.008	—	—	—
97	0.84±0.006	0.85±0.015	9.3±1.0	—
99	0.91±0.004	—	—	—
101	0.90±0.004	0.91±0.087	—	—
Mean	0.83±0.012	0.84±0.019	3.96±0.63	3.8±0.50

= 23), difference between observed eCA across taxonomic groups, with ~3.5-fold higher values in diatom-dominated assemblages relative to *Phaeocystis*-dominated assemblages, and intermediate values in the mixed assemblages.

CO_2 perturbation experiment—The phytoplankton assemblages in our incubation bottles were dominated by diatoms, with *Phaeocystis* accounting for less than 15% of cell abundances in all samples. Predominant diatom genera

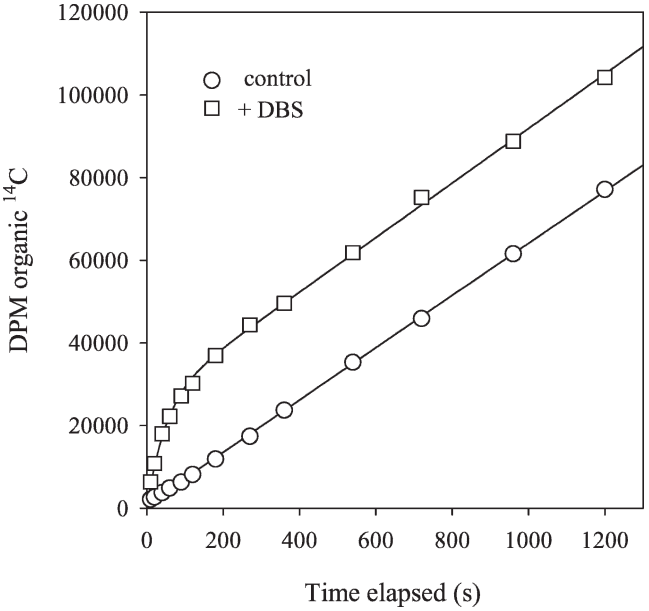

Fig. 3. An example of isotope disequilibrium results in which control experiments do not yield reliable estimates of f or extracellular carbonic anhydrase because of high linearity. Data were obtained with the Ross Sea phytoplankton assemblage at Sta. 95.

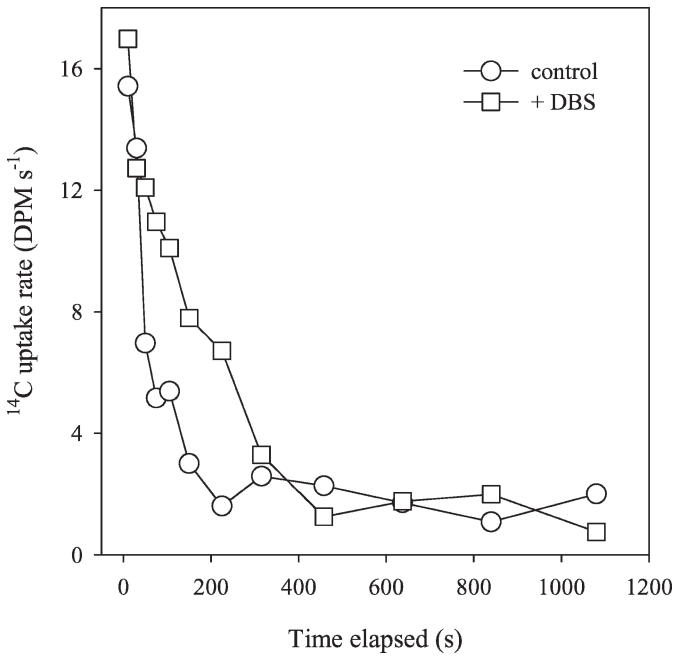

Fig. 4. Instantaneous ^{14}C uptake curves for the phytoplankton assemblage at Sta. 63, showing an enhancement of ^{14}C equilibration in control experiments compared to DBS-treated experiments.

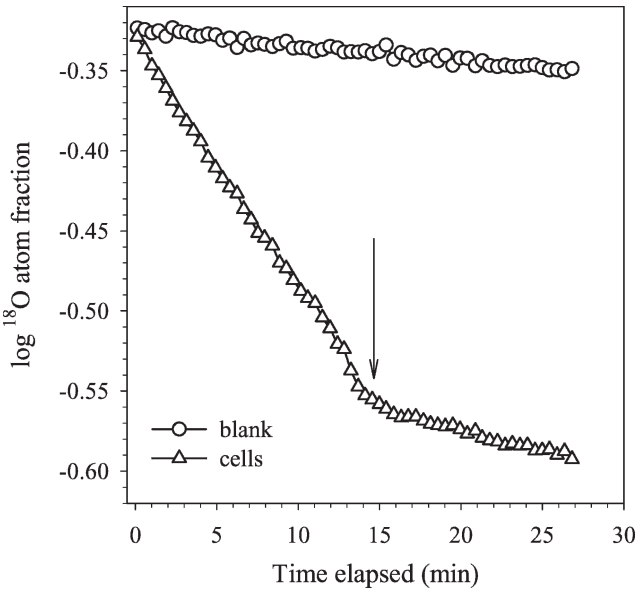

Fig. 5. Typical results of MIMS-based eCA assay with phytoplankton collected at Sta. 63. Arrow shows the time when 100 μmol L^{-1} DBS was added to the cell suspension.

included *Pseudonitzschia*, *Fragilariopsis*, and *Chaetoceros*. At the end of the 8-d period, we did not observe any large CO_2-dependent changes in diatom species composition. Carbon uptake parameters obtained for control experiments (i.e., no DBS additions) are presented in Table 6. The CO_2 manipulations did not have a significant effect either on the fraction of HCO_3^- taken up by cells or on the expression of extracellular carbonic anhydrase as measured by either the isotope disequilibrium experiments or the MIMS analysis (Table 6). There was, however, a large CO_2 effect on short-term ^{14}C fixation rates (i.e., the sum of HCO_3^- and CO_2 uptake; V_t), with higher ^{14}C fixation rates under low CO_2 conditions (Table 6, ANOVA, $p < 0.05$, df = 32).

Discussion

The goal of this study was to examine the pathways of inorganic C uptake by Southern Ocean diatoms and *Phaeocystis*, and to assess the effects of CO_2 variability on C uptake by natural phytoplankton assemblages in the Ross Sea. Our results provide strong evidence for HCO_3^- transport and suggest the presence of CCMs in all of the phytoplankton we examined. To our knowledge, this study represents the first direct comparison of C uptake by natural phytoplankton assemblages and laboratory monocultures. The similarity between laboratory and field results (Fig. 2) is reassuring, and suggests that culture studies of bloom-forming species (Rost et al. 2003) can provide valuable insight into the physiological behavior of phytoplankton assemblages in the oceans.

Table 5. Comparison of C uptake parameters across taxonomically different Ross Sea phytoplankton assemblages.

Dominant phytoplankton	$f\mathrm{HCO}_3^-$*	eCA ^{14}C catalytic enhancement†
Phaeocystis (n=5)	0.81±0.039	2.34±0.32
mixed (n=10)	0.80±0.023	3.89±0.43
diatoms (n=9)	0.88±0.018	8.12±3.07

* ANOVA, df = 23, p>0.05.
† ANOVA, df = 23, p<0.001.

Table 6. Carbon uptake parameters determined for phytoplankton in the CO_2 manipulation experiment.

CO_2 level (Pa)	$f\mathrm{HCO}_3^-$*	V_t DPM (μg Chl a)$^{-1}$ s^{-1}†	Catalytic enhancement*	eCA (U [μg Chl a]$^{-1}$)*
10.1	0.86±0.007	24±0.27	3.6±0.29	2.1±0.15
38.5	0.88±0.014	19±0.31	4.6±0.72	1.8±0.12
81.1	0.87±0.022	16±0.25	5.2±1.0	1.7±0.28

* ANOVA, df=32, p>0.05.
† ANOVA, df=32, p<0.05.

HCO_3^- uptake in the Ross Sea—One of our principal results is the widespread occurrence of HCO_3^- transport among Southern Ocean phytoplankton isolates and Ross Sea phytoplankton assemblages (Tables 3 and 4). In the case of *Phaeocystis*, our C uptake measurements largely reflect the physiological properties of colonies that were present in our laboratory cultures and prevalent in the Ross Sea during the December–January sampling period. Previous work with colonial *Phaeocystis* has demonstrated a large diffusive boundary layer (Ploug et al. 1999), which limits diffusive CO_2 transport to the cell surface and should thus favor HCO_3^- transport. Comparison of our high $f\mathrm{HCO}_3^-$ estimates for colonial *P. antarctica* with the somewhat lower estimates obtained with solitary *Phaeocystis globosa* (Elzenga et al. 2000; Rost et al. 2003) provides support for this hypothesis. In future studies, an explicit comparison of solitary and colonial *Phaeocystis* in the Ross Sea would be of interest, because these respective morphotypes dominate the early and late bloom periods, respectively (Mathot et al. 2000).

Our estimates of HCO_3^- transport in the Ross Sea (~60–90% of total C uptake) are similar to previous values obtained with phytoplankton assemblages in the Bering Sea (Martin and Tortell 2006), subarctic Pacific (Tortell et al. 2006), and equatorial Pacific (Tortell and Morel 2002). In these latter regions, surface water temperatures are considerably higher than in the Ross Sea, and CO_2 solubility correspondingly lower (solubility decreases ~0.5 μmol L^{-1} CO_2 $^\circ$C^{-1}). Previous authors have suggested that the latitudinal gradient in seawater temperature influences phytoplankton C uptake and isotope fractionation by favoring CO_2 uptake in polar waters (Rau et al. 1989). In addition, low temperature increases the intrinsic carboxylase : oxygenase ratio of RubisCO (Badger and Collatz 1977), thus increasing the biochemical CO_2 affinity of photosynthesis and, potentially, decreasing the need for HCO_3^- use. The available field data (present study included) suggest, however, that HCO_3^- uptake by phytoplankton is largely insensitive to ambient surface water temperatures.

Only one previous field study, Cassar et al. (2004), has examined C uptake by phytoplankton assemblages in Antarctic waters. Working with samples collected in the

Polar Frontal Zone, the authors reported a range of $f\mathrm{HCO}_3^-$ values from 0.2 to 0.7 (mean 0.48 ± 0.05), somewhat lower than those we observed in the Ross Sea. Slight methodological differences may account for at least part of this difference. Whereas we used an experimental buffer at pH 8.5, and a CO_2 spike at pH 7.0, Cassar et al. (2004) used unbuffered seawater (pH ~8.2) with a lower HCO_3^- : CO_2 ratio, and a CO_2 spike at pH ~3. In addition, Cassar et al. (2004) employed a somewhat different approach to calculate $f\mathrm{HCO}_3^-$ values, based on estimates of the linearly extrapolated initial and steady-state ^{14}C fixation rates. As discussed by Tortell and Morel (2002), this approach can lead to an underestimation of $f\mathrm{HCO}_3^-$ By comparison, the nonlinear curve-fitting approach we used in our analysis yields $f\mathrm{HCO}_3^-$ estimates that are virtually identical to those derived independently from MIMS-based O_2 and CO_2 flux analysis (Rost et al. 2007). We are thus confident in our HCO_3^- transport estimates.

Methodological discrepancies aside, the physiological explanation for lower apparent HCO_3^- uptake in the Polar Frontal Zone is not presently clear. In principle, acute Fe limitation of phytoplankton productivity in the open Southern Ocean (Boyd 2002) could lead to lower rates of HCO_3^- transport as total cellular C demands decrease. However, the results of Cassar et al. (2004) and other recent studies (Martin and Tortell 2006; Tortell et al. 2006) suggest that HCO_3^- utilization is largely unaffected by changes in Fe availability and primary productivity. Differences in HCO_3^- between Polar Frontal Zone and Ross Sea phytoplankton may thus primarily result from species-specific differences in C uptake among individual phytoplankton. Despite significant variability among field sites, it is clear that HCO_3^- uptake is a common and widespread characteristic of phytoplankton assemblages in a variety of oceanic waters, from equatorial to polar regions.

CO_2-dependent regulation of C transport—Given the resource costs associated with direct HCO_3^- transport (Raven 1991), this process should be down-regulated as ambient CO_2 availability increases. A number of laboratory studies have indeed observed a repression of HCO_3^- transport under high CO_2 culture conditions (Palmqvist et al. 1994; Amoroso et al. 1998), but much of this work has been conducted using very high CO_2 levels (e.g., >1,000 Pa CO_2) whose environmental relevance is questionable. Recently, Rost et al. (2003) have reported a decrease in HCO_3^- uptake by the diatom *Skeletonema costatum* and the coccolithophorid *Emiliania huxleyi* with increasing CO_2 from 3.6, 18.2, 37.5, and 182 Pa. In contrast, *P. globosa* did not regulate inorganic C uptake in response to experimental CO_2 concentrations. The results from our field survey indicate that natural CO_2 gradients in the Ross Sea had little effect on HCO_3^- use by phytoplankton over a range from ~13.2 to 36.5 Pa. This observation is consistent with results obtained in several recent surveys of the Bering Sea (Martin and Tortell 2006), subarctic Pacific (Tortell et al. 2006), and Antarctic Polar Front (Cassar et al. 2004). Moreover, our incubation experiments provide additional evidence for a lack of CO_2 effect on HCO_3^- transport by Ross Sea phytoplankton. Under controlled conditions with similar phytoplankton growth rates and species assemblage composition, the relative fraction of HCO_3^- utilization was virtually identical across an 8-fold CO_2 range (10.1–81.1 Pa CO_2). Collectively, our field results and those of previous studies suggest a constitutive HCO_3^- uptake system in many natural phytoplankton assemblages over the annual range of CO_2 concentrations encountered in oceanic waters.

The absence of a CO_2 effect on HCO_3^- transport does not preclude CO_2-dependent regulation of cellular C uptake kinetics. Rost et al. (2006) observed CO_2 effects on the affinity (i.e., half saturation constants) for photosynthesis and C uptake without large changes in HCO_3^- : CO_2 uptake ratios. Similarly, in our Ross Sea incubation experiments, we observed a CO_2 effect on total short-term C fixation rates (V_t) without an appreciable change in the relative fraction of CO_2 and HCO_3^- utilization (Table 6). This result suggests that phytoplankton respond to low-CO_2 conditions by increasing cellular C transport and/or fixation capacity without altering substrate preference. Similar CO_2-dependent regulation of short-term ^{14}C fixation rates has been reported previously in several field studies (Tortell et al. 2000; Martin and Tortell 2006). These changes indicate that CO_2 availability does indeed influence C acquisition by phytoplankton assemblages in the Ross Sea and other oceanic environments, with cells up-regulating the CCM under low CO_2 conditions.

Carbonic anhydrase activity—In this study, we utilized kinetic analysis of isotope disequilibrium data and MIMS ^{18}O exchange assays to measure eCA. These two methods yield fundamentally different measurements (biomass-normalized bulk activity vs. biomass-independent boundary layer catalysis rates), and are thus not directly comparable (Rost et al. 2007). Nonetheless, our results provide primary evidence for extracellular carbonic anhydrase expression by Ross Sea phytoplankton in situ (Table 4, Fig. 5). To our knowledge, there are no other field data available for direct comparison with our MIMS ^{18}O exchange results. However, the magnitude of our eCA estimates (~1–10 U [μg Chl a]$^{-1}$; Table 4) is similar to that reported by Burkhardt et al. (2001) and Rost et al. (2003) for several laboratory cultures of marine phytoplankton. Note that these previous studies reported eCA as percent enhancement factors (i.e., multiplied by 100), and erroneously reported the units as mg Chl a^{-1} instead of μg Chl a^{-1}.

Several previous field studies have used isotope disequilibrium data to derive eCA for natural phytoplankton assemblages. Comparison of our ^{14}C-based catalytic enhancement factors with these published data suggests that Ross Sea phytoplankton assemblages have somewhat higher extracellular carbonic anhydrase expression levels (mean enhancement 4.0 ± 0.63) than do phytoplankton in the Bering Sea (mean enhancement 2.5 ± 0.29; Martin and Tortell 2006) or subarctic Pacific (mean enhancement 1.4 ± 0.12; Tortell et al. 2006). These apparent regional differences may be partially explained by the effects of seawater temperature on the kinetics of the carbonate system. While aqueous CO_2 solubility increases with

decreasing temperatures (*see* above), the rate of spontaneous HCO_3^- : CO_2 interconversion decreases by approximately 13% $°C^{-1}$. As a result, phytoplankton growing at low ambient temperatures experience much slower rates of spontaneous HCO_3^- to CO_2 interconversion, and would thus experience a larger benefit from the production of extracellular carbonic anhydrase.

It has generally been assumed that extracellular carbonic anhydrase functions to facilitate cellular CO_2 uptake by catalyzing the dehydration of HCO_3^- to CO_2 in the boundary layer. The enzyme may, however, also have a role for cells that predominantly transport HCO_3^-. Indeed, a number of authors have reported a positive correlation between direct HCO_3^- transport and eCA in several diatom species (Burkhardt et al. 2001; Rost et al. 2003; Martin and Tortell 2008). It has been suggested that extracellular carbonic anhydrase could act to scavenge CO_2 that effluxes from cells, rapidly converting it to HCO_3^- in the periplasmic space for subsequent transport across the plasmalemma (Trimborn et al. 2008). Another possibility is the involvement of an extracellular carbonic anhydrase-like moiety in the HCO_3^- transporter (Kaplan and Reinhold 1999). This has been demonstrated convincingly in human erythrocytes (Sterling et al. 2001), but firm molecular evidence is currently lacking for eukaryotic phytoplankton. Further studies will be needed to understand the physiological role of extracellular carbonic anhydrase in cells that predominantly transport HCO_3^-.

As with HCO_3^- transport, extracellular carbonic anhydrase expression by Ross Sea phytoplankton appeared to be only weakly regulated by CO_2 levels, in both field surveys and a direct manipulation experiment. In contrast, several previous field studies have observed clear evidence of CO_2-dependent regulation of extracellular carbonic anhydrase and total cellular CA in other natural phytoplankton assemblages in incubation experiments (Tortell et al. 2002; Martin and Tortell 2006) and along natural CO_2 gradients (Berman-Frank et al. 1994; Tortell et al. 2006). Based on the limited available data, it appears that Ross Sea phytoplankton may be somewhat different than phytoplankton in other oceanic regions, with extracellular carbonic anhydrase expression largely insensitive to ambient CO_2 availability. This apparent constitutive expression of extracellular carbonic anhydrase may be attributable to low surface water temperatures as discussed above.

Comparison of diatoms and Phaeocystis—One of our principal research objectives was to examine the differences in C acquisition among Southern Ocean diatoms and *Phaeocystis*. The motivation for this work came from previous equatorial Pacific results showing an enhancement of *P. pouchetii* biomass relative to diatoms under low CO_2 treatments (Tortell et al. 2002). This result suggested that *Phaeocystis* was better adapted than diatoms to growth under low CO_2 conditions, but the physiological basis for this result was not directly examined. In the Ross Sea, we found that diatom- and *Phaeocystis*-dominated phytoplankton assemblages utilized HCO_3^- to a similar extent, although diatoms appeared to possess higher eCA. We have recently observed similar taxonomic patterns in the Bering Sea, where diatoms possessed higher eCA than other phytoplankton groups (mostly nanoflagellates), with no clear differences in relative HCO_3^- transport rates (Martin and Tortell 2006). At present, it is unclear how the observed differences in extracellular carbonic anhydrase expression among phytoplankton might influence their competitive responses to natural and anthropogenic CO_2 variability. Additional physiological data are needed to fully assess the energetic efficiency and resource costs of the CCM. In particular, information is needed on the kinetic properties (i.e., V_{max} and K_m) of the C transport system in a range of diatoms and *Phaeocystis*, the rates of gross vs. net C uptake, and the effects of variable light regimes on C uptake (Rost et al. 2006).

Our underway surveys did not reveal any strong spatial patterns in the distribution of phytoplankton taxa with respect to ambient CO_2 levels in the Ross Sea. While the waters lowest in CO_2 (<20.3 Pa) occurred in diatom-dominated regions, *Phaeocystis* blooms also occurred under conditions of significant CO_2 undersaturation. Unfortunately, *Phaeocystis* was not abundant in the water we collected for our incubation experiment, and we were thus unable to specifically examine CO_2 effects on diatom and *Phaeocystis* dominance. Over the relatively short time frame of our incubation experiment, we did not observe any large difference in diatom species composition across the CO_2 treatments. However, in longer experiments (>10 d) we have observed significant CO_2-dependent diatom species shifts in Ross Sea phytoplankton assemblages (Tortell et al. 2008). In these experiments, phytoplankton cultured with low CO_2 were dominated by thin pennate diatoms of the genus *Pseudonitzschia*, whereas large species of *Chaetoceros* became abundant under high-CO_2 conditions. The high surface area to volume ratios of the *Pseudonitzschia* would provide an advantage under low CO_2, where cells appear to up-regulate total C uptake rates. Our preliminary observations suggest that CO_2 concentrations can indeed influence phytoplankton species dynamics in the Ross Sea. Future field and laboratory studies are needed to fully elucidate the physiological ecology underlying this important result.

Our work also bears direct relevance to the interpretation of stable C isotope signatures of particulate organic carbon in the Ross Sea and other Antarctic marginal seas dominated by diatoms and *Phaeocystis*. Previous studies have suggested significant differences in C isotope fractionation by Ross Sea diatoms and *Phaeocystis*, with the latter group exhibiting lower ^{13}C : ^{12}C ratios (Villinski et al. 2000). One interpretation of this result is that diatoms transport more HCO_3^- than *Phaeocystis*, because HCO_3^- is ~10‰ enriched in ^{13}C relative to the aqueous CO_2 pool (Mook et al. 1974). Our results indicate, however, that differences in relative HCO_3^- utilization cannot explain the unique C isotope signatures of these groups. Similarly, differences in eCA should not affect cellular C isotope fractionation, because this enzyme merely acts to catalyze HCO_3^- : CO_2 interconversion without altering equilibrium concentrations or isotope fractionation between these carbon species. The ^{13}C enrichment in diatoms may thus be attributable to lower rates of C efflux in diatoms, or

possibly to the contribution of a C_4 photosynthetic pathway in this group. Further work will be needed to critically evaluate these possibilities.

References

Amoroso, G., D. Sültemeyer, C. Thyssen, and H. P. Fock. 1998. Uptake of HCO^-_3 and CO_2 in cells and chloroplasts from the microalgae *Chlamydomonas reinhardtii* and *Dunaliella tertiolecta*. Plant Physiol. **116:** 193–201.

Arrigo, K. R., D. H. Robinson, D. L. Worthen, R. B. Dunbar, G. R. Ditullio, M. Vanwoert, and M. P. Lizotte. 1999. Phytoplankton community structure and the drawdown of nutrients and CO2 in the Southern Ocean. Science **283:** 365–367.

———, and G. L. van Dijken. 2004. Annual changes in sea-ice, chlorophyll a, and primary production in the Ross Sea, Antarctica. Deep-Sea Res. II **51:** 117–138.

———, and ———. 2007. Interannual variation in air-sea CO_2 flux in the Ross Sea, Antarctica: A model analysis. J. Geophys. Res. Oceans **112:** C03020, doi:10.1029/2006JC003492.

Badger, M. R., and G. J. Collatz. 1977. Studies on the kinetic mechanism of ribulose-1,5-bisphosphate carboxylase and oxygenase reactions, with particular reference to the effect of temperature on kinetic parameters. Carnegie Inst. Wash. Year Book **76:** 355–361.

———, and G. D. Price. 1989. Carbonic anhydrase activity associated with the cyanobacterium Synechococcus PCC7942. Plant Physiol. **89:** 51–60.

Bates, N. R., D. A. Hansell, C. A. Carlson, and L. I. Gordon. 1998. Distribution of CO_2 species, estimates of net community production, and air-sea CO_2 exchange in the Ross Sea polynya. 1998. J. Geophys. Res. Oceans **103:** 2883–2896.

Berman-Frank, I., T. Zohary, J. Erez, and Z. Dubinsky. 1994. Carbonic anhydrase and the annual dinoflagellate bloom in Lake Kinneret. Limnol. Oceanogr. **39:** 1822–1834.

Boyd, P. W. 2002. Environmental factors controlling phytoplankton processes in the Southern Ocean. J. Phycol. **38:** 844–861.

Burkhardt, S., G. Amoroso, U. Riebesell, and D. Sültemeyer. 2001. CO_2 and HCO^-_3 uptake in diatoms acclimated to different CO_2 concentrations. Limnol. Oceanogr. **46:** 1378–1391.

Cassar, N., E. A. Laws, R. R. Bidigare, and B. N. Popp. 2004. Bicarbonate uptake by Southern Ocean phytoplankton. Global Biogeochem. Cycles **18:** GB3003, doi:10.1029/2003GB002116.

Debaar, H. J. W., J. T. M. Dejong, D. C. E. Bakker, B. M. Loscher, C. Veth, U. Bathmann, and V. Smetacek. 1995. Importance of iron for plankton blooms and carbon-dioxide drawdown in the Southern-Ocean. Nature **373:** 412–415.

Ditullio, G. R., and others. 2000. Rapid and early export of *Phaeocystis antarctica* blooms in the Ross Sea, Antarctica. Nature **404:** 595–598.

Elzenga, J. T. M., H. B. A. Prins, and J. Stefels. 2000. The role of extracellular carbonic anhydrase activity in inorganic carbon utilization of *Phaeocystis globosa* (Prymnesiophyceae): A comparison with other marine algae using the isotopic disequilibrium technique. Limnol. Oceanogr. **45:** 372–380.

Espie, G. S., and B. Colman. 1986. Inorganic carbon uptake during photosynthesis 1. A theoretical analysis using the isotopic disequilibrium technique. Plant Physiol. **80:** 863–869.

Giordano, M., J. Beardall, and J. A. Raven. 2005. CO_2 concentrating mechanisms in algae: Mechanisms, environmental modulation, and evolution. Annu. Rev. Plant Biol. **56:** 99–131.

Gordon, L. I., J. C. Jennings Jr., A. A. Ross, and J. M. Krest. 1993. A suggested protocol for continuous flow automated analysis of seawater nutrients (phosphate, nitrate, nitrite and silicic acid) in the WOCE Hydrographic Program and the Joint Global Ocean Fluxes Study. WHP Office Report WHPO 91-1. WOCE Reports No. 68/91.

Hein, M., and K. Sand-Jensen. 1997. CO_2 increases oceanic primary production. Nature **388:** 526–527.

Kaplan, A., and L. Reinhold. 1999. CO_2 concentrating mechanisms in photosynthetic microorganisms. Annu. Rev. Plant Physiol. Plant Mol. Biol. **50:** 539–559.

Keller, M. D., W. K. Bellows, and R. L. Guillard. 1989. Dimethylsulfide production in marine phytoplankton, p. 167–182. *In* E. S. Salztman and W. J. Cooper [eds.], Biogenic sulfur in the environment. American Chemical Society.

Martin, C. L., and P. D. Tortell. 2006. Bicarbonate transport and extracellular carbonic anhydrase activity in Bering Sea phytoplankton assemblages: Results from isotope disequilibrium experiments. Limnol. Oceanogr. **51:** 2111–2121.

———, and ———. 2008. Bicarbonate transport and extracellular carbonic anhydrase in marine diatoms. Physiol. Plant. **133:** 106–116.

Mathot, S., W. O. Smith, C. A. Carlson, D. L. Garrison, M. M. Gowing, and C. L. Vickers. 2000. Carbon partitioning within *Phaeocystis antarctica* (Prymnesiophyceae) colonies within the Ross Sea, Antarctica. J. Phycol. **36:** 1049–1056.

Mitchell, C., and J. Beardall. 1996. Inorganic carbon uptake by an Antarctic sea-ice diatom, Nitzschia frigida. Polar Biol. **16:** 95–99.

Mook, W. G., J. C. Bommerso, and W. H. Staverma. 1974. Carbon isotope fractionation between dissolved bicarbonate and gaseous carbon dioxide. Earth Planet. Sci. Lett. **22:** 169–176.

Palmqvist, K., J. W. Yu, and M. R. Badger. 1994. Carbonic anhydrase activitiy and inorganic carbon fluxes in low Ci and high Ci cells of *Chlamydomonas reinhardtii* and *Secendesmus obliquus*. Physiol. Plant. **90:** 537–547.

Parsons, T. R., Y. Maita, and C. M. Lalli. 1984. A manual of chemical and biological methods for seawater analysis. Pergamon.

Ploug, H., W. Stolte, E. H. G. Epping, and B. B. Jorgensen. 1999. Diffusive boundary layers of the colony-forming plankton alga *Phaeocystis* sp.—implications for nutrient uptake and cellular growth. Limnol. Oceanogr. **44:** 1959–1967.

Price, N. M., G. I. Harrison, J. G. Hering, R. M. Hudson, P. M. V. Nirel, B. Palenik, and F. M. M. Morel. 1988. Preparation and chemistry of the artificial algal culture medium AQUIL. Biol. Oceanogr. **6:** 443–461.

Rau, G. H., T. Takahashi, and D. J. D. Marais. 1989. Latitudinal variations in plankton delta-C-13—implications for CO_2 and productivity in past oceans. Nature **341:** 516–518.

Raven, J. A. 1991. Physiology of inorganic carbon acquisition and implications for resource use efficiency by marine phytoplankton: Relation to increased CO_2 and temperature. Plant Cell Environ. **14:** 779–794.

Reinfelder, J. R., A. J. Milligan, and F. M. M. Morel. 2004. The role of the C-4 pathway in carbon accumulation and fixation in a marine diatom. Plant Physiol. **135:** 2106–2111.

Riebesell, U., D. A. Wolf-Gladrow, and V. Smetacek. 1993. Carbon dioxide limitation of marine phytoplankton growth rates. Nature **361:** 249–251.

Rost, B., U. Riebesell, S. Burkhardt, and D. Sültemeyer. 2003. Carbon acquisition of bloom-forming marine phytoplankton. Limnol. Oceanogr. **48:** 55–67.

———, ———, and D. Sültemeyer. 2006. Carbon acquisition of marine phytoplankton: Effect of photoperiod length. Limnol. Oceanogr. **51:** 12–20.

———, S. A. Kranz, K. U. Richter, and P. D. Tortell. 2007. Isotope disequilibrium and mass spectrometric studies of inorganic carbon acquisition by phytoplankton. Limnol. Oceanogr. Methods **5:** 328–337.

Schlitzer, R. 2002. Carbon export fluxes in the Southern Ocean: Results from inverse modeling and comparison with satellite-based estimates. Deep-Sea Res. II **49:** 1623–1644.

Sedwick, P. N., and G. R. Ditullio. 1997. Regulation of algal blooms in Antarctic shelf waters by the release of iron from melting sea ice. Geophys. Res. Lett. **24:** 2515–2518.

Sigman, D. M., and E. A. Boyle. 2000. Glacial/interglacial variations in atmospheric carbon dioxide. Nature **407:** 859–869.

Smith, W. O., R. F. Anderson, J. K. Moore, L. A. Codispoti, and J. M. Morrison. 2000. The U.S. Southern Ocean Joint Global Ocean Flux Study: An introduction to AESOPS. Deep-Sea Res. II **47:** 3073–3093.

———, and V. L. Asper. 2001. The influence of phytoplankton assemblage composition on biogeochemical characteristics and cycles in the southern Ross Sea, Antarctica. Deep-Sea Res. I **48:** 137–161.

Sterling, D., R. A. F. Reithmeier, and J. R. Casey. 2001. Functional interaction of carbonic anhydrase II and chloride/bicarbonate exchangers. J. Biol. Chem. **276:** 47886–47894.

Tortell, P. D. 2005. Dissolved gas measurements in oceanic waters made by membrane inlet mass spectrometry. Limnol. Oceanogr. Methods **3:** 24–37.

———, G. R. Ditullio, D. M. Sigman, and F. M. M. Morel. 2002. CO_2 effects on taxonomic composition and nutrient utilization in an equatorial Pacific phytoplankton assemblage. Mar. Ecol. Prog. Ser. **236:** 37–43.

———, C. L. Martin, and M. E. Corkum. 2006. Inorganic carbon uptake and intracellular assimilation by subarctic Pacific phytoplankton assemblages. Limnol. Oceanogr. **51:** 2102–2110.

———, and F. M. M. Morel. 2002. Sources of inorganic carbon for phytoplankton in the eastern Subtropical and equatorial Pacific Ocean. Limnol. Oceanogr. **47:** 1012–1022.

———, G. H. Rau, and F. M. M. Morel. 2000. Inorganic carbon acquisition in coastal Pacific phytoplankton communities. Limnol. Oceanogr. **45:** 1485–1500.

———, and others. 2008. The CO_2 sensitivity of Southern Ocean phytoplankton. Geophysical Research Letters, Geophys. Res. Lett. **35:** L04605, doi:10.1029/2007GL032583.

Trimborn, S., N. Lundholm, S. Thoms, K. U. Richter, B. Krock, P. J. Hansen, and B. Rost. 2008. Inorganic carbon acquisition in potentially toxic and non-toxic diatoms: The effect of pH induced changes in seawater carbonate chemistry. Physiol. Plant. **133:** 92–105.

Villinski, J. C., R. B. Dunbar, and D. A. Mucciarone. 2000. Carbon 13/carbon 12 ratios of sedimentary organic matter from the Ross Sea, Antarctica: A record of phytoplankton bloom dynamics. J. Geophys. Res. **105:** 14163–14172.

Received: 12 October 2007
Accepted: 9 March 2008
Amended: 28 March 2008